

Article

The Concept of Optimal Compaction of the Charge in the Gravitation System Using the Grains Triangle for Cokemaking Process

Andrzej Mianowski , Bartosz Mertas  and Marek Ściażko 

Institute for Chemical Processing of Coal, Zamkowa 1, 41-803 Zabrze, Poland; amianowski@ichpw.pl (A.M.); msciazko@ichpw.pl (M.Ś.)

* Correspondence: bmertas@ichpw.pl; Tel.: +48-32-621-2244

Abstract: Two isomorphic sets of grains, small and large, were analysed—without specifying their dimensions—under the acronym CMC (Curve of Maximum Compression) and taking into account the effects of segregation CMCS. The proposal is particularly valuable for optimal blend preparation in the gravity system in cokemaking. The main advantage of this work is the proposal of using the grains triangle, which limits the values calculated by the relations: bulk density-share of coarse/fine grains, for different levels of moisture content. Each system of changing shares of coarse grains is characterised by a constant C, but there is no need to determine it. Compliance of the calculated value with the experimentally determined value means that the given arbitrary grain set has reached its maximum density called the “locus”. The grains triangle practically covers the vast majority of laboratory and industrial test results, and geometrically or computationally indicates the ability of a given particle size distribution to reach maximum bulk density. This paper presents analysis of the results of tests on crushing, coal briquettes, and grinding coal blend in selected mechanical systems. Results of tests on coke quality (CRI, CSR) in connection with the grain size triangle are discussed.

Keywords: coal; bulk density; porosity; coefficient of susceptibility; grains triangle; coke quality



Citation: Mianowski, A.; Mertas, B.; Ściażko, M. The Concept of Optimal Compaction of the Charge in the Gravitation System Using the Grains Triangle for Cokemaking Process. *Energies* **2021**, *14*, 3911. <https://doi.org/10.3390/en14133911>

Academic Editor: Manoj Khandelwal

Received: 19 May 2021

Accepted: 24 June 2021

Published: 29 June 2021

Publisher's Note: MDPI stays neutral with regard to jurisdictional claims in published maps and institutional affiliations.



Copyright: © 2021 by the authors. Licensee MDPI, Basel, Switzerland. This article is an open access article distributed under the terms and conditions of the Creative Commons Attribution (CC BY) license (<https://creativecommons.org/licenses/by/4.0/>).

1. Introduction

The coking process in classical coke oven batteries is invariably material- and energy-consuming. Of the two known charging systems for the coking process, at present stamping (apart from top charged) seems to be a more prospective solution due to the use of weaker coking coals with an increased content of semi-soft coal [1]. In turn, top charging requires coals with very good coking properties (hard coal), but is technologically less complicated. For that reason, it is still used and there are several possibilities for this variant to intensify the coking process. Due to the capital expenditure, very expensive method is to dry the charge to the level of 5% moisture [2] (less often used for even more expensive charge pre-heating), followed by briquetting part of the charge 30–40% [3] (less frequently granulating), using charge additives (oiling or coking substances [4]), and rational selection of particle size distribution, including selective crushing [5].

Optimal selection of the grain composition for specific raw materials and technological possibilities is a very significant opportunity to improve the quality of coke on the NSC index scale, which was confirmed during tests conducted by IChPW (Figure 1—item 1).

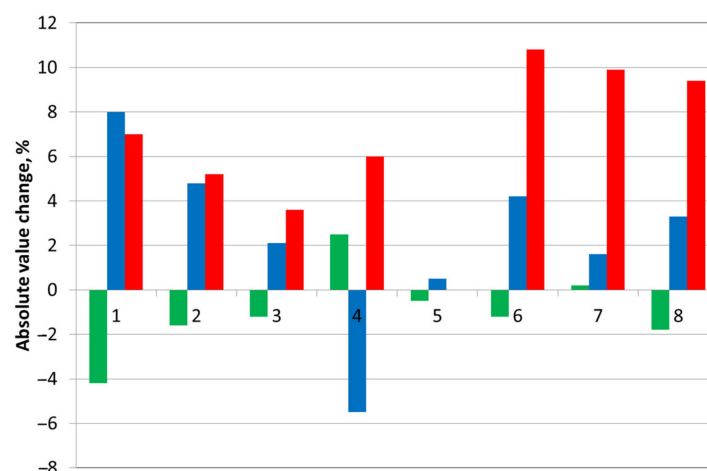


Figure 1. Absolute changes in coke quality indices CSR (green) and CRI (blue), and % change (increase) of the bulk density (red): (1) selective crushing, (2) pre-drying, (3) tar—water emulsion addition, (4) granulation (3% addition of tar—water emulsion), (5) leaning additives (3% pet-coke), (6) vibrating densification (3% addition of tar—water emulsion), (7) pre-drying = briquetting, (8) pre-drying + vibrating densification (3% addition of tar—water emulsion). Source: authors own work based on [6,7].

Analysing the possibilities for increasing the production capacity in gravity-charged coke oven batteries, the rules defining the degree of fineness of the coal blend are generally known. However, in this system, with the rational selection of grains intended for the coking process, the differences in bulk density between the upper and lower limits of real grain sizes can be over 20 kg/m^3 [8].

The increase in bulk density not only increases the production capacity of the battery, but also in some areas of coal grain size distribution, it positively influences the quality of coke, demonstrating a linear, beneficial effect of bulk density on the quality indicators of CRI and CSR coke [7,9].

In general, the grain size distribution of the coal blend for the gravity system is limited by specific technological guidelines. The most frequent is the share of grains larger/smaller than 3 mm and the proportion of fine grains less than 0.5 mm, aiming for the lowest possible, as well as a total moisture content below 10%.

Practice shows that for the top charging system, the grinding degree, as a share of grains below 3 mm, is 73–87%, with the proportion of the dust fraction being no greater than 42%.

Research conducted using a planned experiment indicates that for a moisture content of $W_{ex}^r = 6\text{--}8\%$, the maximum compaction is obtained for the grains of two grain sets 0.5–1 mm and over 3 mm in an approximate 1:1 ratio [10].

Practically fine grains, below 0.5 mm at this moisture level, are unfavourable. Such idealised expectations in this respect due to coal mine production reasons are impossible for daily implementation.

Research on bulk density development due to the ability to achieve grains compaction of variable size and shape consists in predicting the filling of free interstitial spaces of the skeleton of grains defined as thick. They constitute a structural framework. For the sake of simplicity, the most common arrangement is a spherical grain (shape factor $f = 1$). Theoretically, at least two, and usually more, isomorphic components of dry grains are analysed, creating model mixtures with a given bulk density by computational or experimental method according to the planned experiment. Approaches to this issue are very different; there are known theses of Simonis et al. [11,12], the approach according to the granulometric parameter method [13–15], and the concepts of Strugala [10,16–18].

In 1989, the Curve of Maximum Compression (CMC) model was proposed, and if it considers the segregation effects, the acronym CMCS is used [19].

2. CMC and CMCS Models

According to [19], CMC is a system of two equations relative to shares, which assume isomorphic dimensions of fine (x_d) and coarse (x_g) grains in a fairly free manner. Small grains fill the structural skeleton composed of coarse grains, where: $x_d + x_g = 1$, and one assumes knowledge of their real density ρ_o :

$$\frac{\rho}{\rho_o} = \frac{\pi}{6} \cdot \frac{1}{1 - x_d}, \quad 0 \leq x_d \leq x_d^* = \frac{1 - \frac{\pi}{6}}{2 - \frac{\pi}{6}} \quad (1a)$$

$$\frac{\rho}{\rho_o} = \frac{\pi}{6} \cdot \frac{1}{\frac{\pi}{6} + (1 - \frac{\pi}{6}) \cdot x_d}, \quad x_d^* \leq x_d \leq 1 \quad (1b)$$

At the intersection of two branches of curves (1), the maximum bulk density is:

$$\frac{\rho^*}{\rho_o} = \frac{\pi}{6} \left(2 - \frac{\pi}{6} \right) \quad (2)$$

and the maximum relative bulk density increase is:

$$\frac{\Delta \rho}{\rho} = 1 - \frac{\pi}{6} = \varepsilon_o = 0.4765 \quad (3)$$

Then, both Equation (1a,b) are transformed into a CMCS model with the form containing only one C constant, defined as the grain division constant:

$$\frac{\rho}{\rho_o} = \frac{\pi}{6} \frac{1 + C(1 - x_d)}{1 + C(1 - x_d)^2} \quad \text{where } x_d = 1 - x_g \quad (4)$$

The practical use of Equation (4) requires a re-analysis of the model Equation (1a,b).

3. Aim of the Work

The aim of the present work is to perform an in-depth analysis of the correctness of Equations (1a,b) and (4) for real systems with different initial mono-fraction bulk densities by taking into account the split grain size. The generalisation leads to the proposal of new variables in the 2D system, taking into account any grain sets and with variable moisture content. Such a diagram is called the grain size triangle. The CMC and CMCS models were used to assess the processes of crushing coal briquettes and grinding the coal mixture. Grain size triangle was used to assess the quality of coke in the coking trials in the laboratory coking installation Karbotest [20] and the possibility of preparing the coal blend for coking. This work presents variants and experimental considerations regarding grain size distribution influence on charge density at first and consecutively on coke quality. While the processes or unit operations leading to the grain size change in coke production can be easily imagined a priori, the assigned models presented in Table 1 have been established ex post. In particular, the grains triangle, which is an original input of this work, is of importance. The adopted order (Table 1) results from the complexity of the model approach and not of technological significance.

Table 1. Models describing the grain system.

| Grain Size Triangle (Equations (15) and (23)) | Models | Processes, Unit Operations |
|--|---|--|
| no | CMC, Equation (1a) | coarse grains (briquettes) crushing, $D_g \gg D_d$ |
| yes | CMCS, Equations (14) and (25) | coal charge crushing, $D_g \rightarrow D_d$ |
| yes | GGs, Equation (40) | pre-drying, $W_i^r = 10 \rightarrow 4\%$ |
| yes | - | pilot coking test (Karbotest installation) |
| yes | ρ vs. x_g , 3rd degree polynomial, Equations (32), (34) and (39) | literature data from experimental design |

4. Variant Considerations (CMC and CMCS Models and Split Grain Size)

4.1. Grain Size Triangle and Possible Variants

The CMC model is very simple, so critical analyses are justified if the assumed considerations are absolutely undisputed. According to [18], with the arrangement of two isomorphic spheres, at least five variants of the arrangement of such grain sets can be imagined. If we add spheres with intermediate dimensions to it, then structures may be created in which the role of small grains will be taken over by the dimensions temporarily considered thick [21].

The CMC model can be further developed using the identity of isomorphic spheres (see Equation (2)):

$$1 - \frac{\pi}{6} = \varepsilon_o \quad \text{or} \quad 1 - \varepsilon_o = \frac{\pi}{6} \quad (5)$$

thanks to which Equation (1a) for the participation of only coarse grains ($x_d = 0$) is recorded as:

$$\frac{\rho}{\rho_o} = 1 - \varepsilon_o, \quad \text{mono-fraction} \quad (6)$$

Further, we add fine grains until saturation, and so we write Equation (2) as:

$$\frac{\rho}{\rho_o} = 1 - \varepsilon_o + (1 - \varepsilon_o)\varepsilon_o = 1 - \varepsilon_o^2, \quad \text{two fractions, coarse and fine grains} \quad (7)$$

This ends the validity of Equation (1a) for $\rho = \rho^*$.

For these considerations, we add further isomorphic spheres, but smaller than fine grains are formed in the amount of a finite geometric series with progress constant $0 < \varepsilon_o < 1$, $\varepsilon_o = 0.4765$, for

$$\frac{\rho}{\rho_o} = 1 - \varepsilon_o + (1 - \varepsilon_o)\varepsilon_o + (1 - \varepsilon_o)\varepsilon_o^2 \quad (8)$$

Equation (8) can be written in the form

$$\frac{\rho}{\rho_o} = (1 - \varepsilon_o)(1 + \varepsilon_o + \varepsilon_o^2) \quad (9)$$

which is:

$$\frac{\rho}{\rho_o} = 1 - \varepsilon_o^3 = 0.892 \quad (10)$$

Equations (8)–(10) describe three fractions: coarse, fine, and very fine grains.

For added smaller and smaller grains with geometrical dimensions suited to free spaces, Equation (10) tends to $\frac{\rho}{\rho_o} = 1$ ($\frac{\rho}{\rho_o} = 1 - \varepsilon_o^p$, $p \rightarrow \infty$), which corresponds to an unattainable boundary condition for the free laying of a series of balls in a given volume.

In the discussed Equations (1a,b), (4) and (6)–(10), the size of the split grain size is not given, and only the term fine and coarse grains is used.

According to the considerations of Simonis [11], the minimum ratio of fine to coarse grain diameters should be $D_d/D_g = (\sqrt{2} - 1) = 0.4142$. Table 2 presents other possibilities in this respect for the two grain fractions. In particular, this is shown in items No. 2 (related to No. 1) and 3. The ratio No. 1 can be adjusted for the CMC model, Equation (1a,b). For this purpose, we compare Equation (7) and Equation (1a) or Equation (1b) for one large ball (diameter D_g) and eight smaller balls (D_d). For a less complicated calculation, we use Equation (1a) and we obtain:



$$1 - \varepsilon_o^2 = \frac{\pi}{6} * \frac{1}{x_g} \quad (11)$$

where

$$\frac{1}{x_g} = 1 + 8\left(\frac{D_d}{D_g}\right)^3 \quad (12)$$

which leads to the wanted relation: $D_d/D_g = (\frac{\epsilon_0}{8})^{1/3} = 0.3905 < \sqrt{2} - 1$.

Table 2. Diameter for two fractions, coarse (g) and fine (d) grains.

| | $\frac{D_d}{D_g} =$ | $\frac{\rho}{\rho_0} = 1 - \epsilon$ | Vision | Conditions | Remarks | Dividing Grain for $D_g = 10$ mm |
|---|--|--|---|--|---|----------------------------------|
| 1 | $\sqrt{2} - 1 = 0.4142$ | 0.8213 |  | $D_d = D_g \cdot (\sqrt{2} - 1) = D_g \cdot 0.414$ | exceeds max Simonis [11] | 4.142 mm |
| 2 | $\sqrt{2} - 1.024 = 0.3902$ | 0.7725 | correction using Equation (2) | $D_d = 0.390 \cdot D_g$ | ~max | 3.902 mm |
| 3 | $\frac{\sqrt{6}}{2} - 1 = 0.2247$ | 0.5711 |  | $D_d = 0.225 \cdot D_g$ | exceeds max Bryczkowski [22], Figure 2b | 2.247 mm |
| 4 | $\sqrt[3]{\frac{1-\frac{\pi}{6}}{8}} = 0.3905$ | $\frac{\pi}{6} (2 - \frac{\pi}{6}) = 0.7730$ | | | Equations (11) and (12) and max acc. Equation (2) | Average 3.43 mm |

The case of No. 3 (Figure 2) is more complicated and includes spheres of smaller and smaller diameter, and then the greatest packing occurs when the spheres touch each other and their centres occupy positions at the corners of a regular tetrahedron. However, it should be kept in mind that this is a rare case. To a certain extent, such an arrangement is observed with the gravitational flow of granular material, and it is a favourable phenomenon when a sequence of smaller and smaller grains is forced into the space of the coarse grain system. An example is the top charged system at a coke plant when during chamber filling with coal, cones are formed before mechanical levelling of the charge. We always observe allocation of mass gradients where the highest density occurs in the chamber sole.

Figure 2b shows that filling coarse grains with smaller grains causes an increase in density slightly higher than the level of $\rho/\rho_0 = 0.7405$ to the value of $\rho/\rho_0 = 0.7909$.

Exceeding densification in relation to Equation (2) is the result of adopting a tetrahedron volume as a limitation, different from the one for which the CMC model was derived ($\rho/\rho_0 = 1 - \epsilon_0^2 = 0.7730$).

For coking in the top charged system, the largest grain of 10 mm coal blend can be adopted in further considerations, because the share of grains in the coking chamber with dimensions above 10 mm is below 5%, and occasionally up to 10%.

Assuming that the largest large grain has the dimensions $D_g = 10$ mm, then the mean subdivision grain is 3.43 mm (Table 2), so the assumption of the split grain size equal to 3 mm is justified.

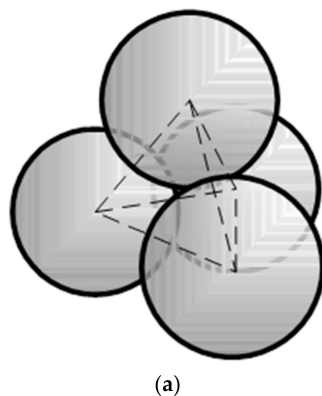


Figure 2. Cont.

From the considerations in Equation (16), there are also other possibilities presented in Table 2.

Therefore, in the ideal case, the straight line, or actually the ray in Equation (14) reaches the highest value at the maximum point, and the coordinate [0; 0] is common to both edge nodes.

For coal intended for coking $\rho_0 = 1300 \text{ kg/m}^3$, although according to [18] this density is variable and slightly exceeds the accepted state, i.e., $\rho_0 = 1319 \div 1326 \text{ kg/m}^3$, which undoubtedly has a connection with the share of mineral substance.

For the assumption under consideration, the arrangement of functional scales (15) is expressed as follows:

$$a\rho^d - 1 = Cx_g(1 - a\rho^d x_g) \quad (17)$$

From Equation (17), the possibility of calculating the division constant of grains follows directly:

$$C = \frac{a\rho^d - 1}{x_g(1 - a\rho^d x_g)} \quad \text{where } a = \frac{6}{\pi\rho_0} = 0.00147 \quad (18)$$

For relation (13), the function has a maximum for the condition $\frac{d\rho^d}{dx_g} \equiv 0$ and we obtain the coordinates for the maximum bulk density:

$$\rho^* = \frac{\pi}{6}\rho_0 \frac{C\sqrt{1+C}}{2(1+C - \sqrt{1+C})} \quad (19)$$

for

$$x_g^* = \frac{\sqrt{1+C} - 1}{C}, \quad \text{where } C > 0 \quad (20)$$

Referring to the present experience, in theory the constant C assumes values from the interval $0 < C < C_{\max} = 1.791$, practically covering the range $0.2 < C < 1.791$. For the volume of coking chambers of a top charging system, the grain division constant is in the order of $C = 0.4$, while in laboratory tests (for a mass of approx. 4 kg of coal) it is much higher, in the order of $C = 0.5 - 1.5$.

Going further in this aspect, from the formulas (19) and (20) we obtain specific coordinate values $[x_g^*; \rho^*]$, which we convert into coordinates of the functional scale system (15), i.e.:

$$Y^* = a\rho^* - 1 \quad (21)$$

$$X^* = x_g^* (1 - a\rho^* x_g^*) \quad \text{or} \quad X^* = x_g^* [1 - (Y^* + 1)x_g^*] \quad (22)$$

Transformed data according to (21) and (22) form a linear relationship, i.e., locus of maximum value, hereinafter referred to as locus (23):

$$Y^* = -5.559X^* + 1.366 \quad (r^2 = 0.9957) \quad (23)$$

Locus (23) is the fundamental point of prediction of the search for the maximum density of the grain system in a given dimensional class characterised by the constant C .

Figure 3a shows the CMCS model and its linear transformation and locus (23), which determines the maximum bulk density, and Figure 3b is a graphic representation of the wanted solution.

This is called the triangle of grain size.

Most of the test results are in the field of this grain size triangle.

The maximum bulk densities are therefore information about the expected purpose of the search.

Models require the number of coarse grains responsible for the existence of the maximum in the CMCS model given in Table 3 in items No. 2 and 3. However, the inequality

(16) and Equation (13) is satisfied when: $0 \leq x_g \leq 1$. The necessary quantity of coarse grains increases as the compaction becomes weaker and weaker, as this is a situation leading to a mono-fraction. The CMCS model (13) reduced to the linear form Equation (14) indicates that the lowest coordinate of the maximum for the weakest compaction $C = 0.2$ is $X^* = \sim 0.24$. Resolving the $[X^*; CX^*]$ coordinates for $C = C_{\max}$ and $C = 0.2$ twice gives the locus (23) again. In particular, the line passing through the two points $[0.1872; 0.3353]$ and $[0.2386; 0.0477]$ gives the equation:

$$Y^* = -5.594X^* + 1.383 \quad (24)$$

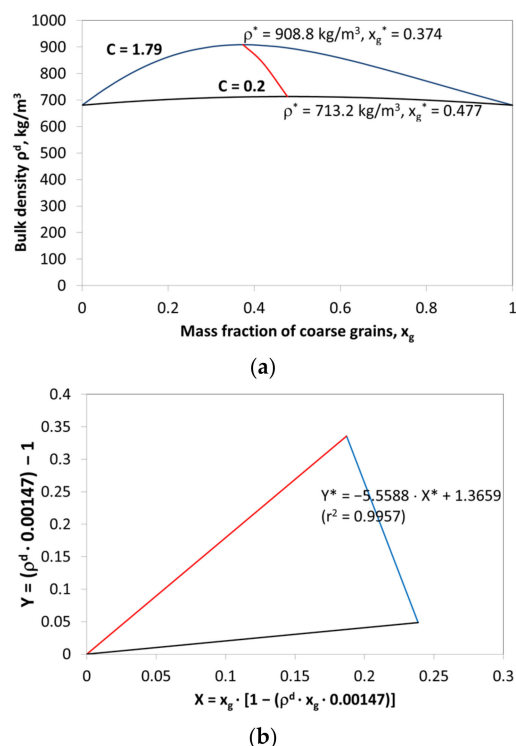


Figure 3. Relationships between bulk density and share of coarse grains above 3 mm: (a) dependence in Cartesian coordinate system for $C = 0.2$ (black), $C = 1.79$ (red), and locus (23) (blue); (b) transformation acc. (15) from the locus (blue) for two C values as in Figure 3a.

Table 3. Variation range of coarse grains share, $0 \leq x_g \leq \frac{\pi \rho_o}{6 \rho^d}, \frac{\pi}{6} = 1 - \varepsilon_o$.

| No | $\frac{\rho}{\rho_o} =$ | $x_g \leq$ | $x_g \leq$ | New Variable in Maximum Y^* | X^* | Remarks |
|-----------|--|---|------------|--|---|--|
| 1 CMC | $1 - \varepsilon_o^2 = 0.7730$ Equation (7) | $(2 - \frac{\pi}{6})^{-1}$ Equations (5) and (7) | 0.6773 | - | - | two fractions, coarse and fine grains |
| 2 CMCS | $\frac{\pi}{12} \frac{C\sqrt{1+C}}{1+C-\sqrt{1+C}}$ Equation (19) | $2 \frac{1+C-\sqrt{1+C}}{C\sqrt{1+C}}$ | 0.7489 | $\frac{1}{2} \frac{C\sqrt{1+C}}{1+C-\sqrt{1+C}} - 1$ $Y^* = C * X^*$ Equation (15) | $\frac{\sqrt{1+C}-1}{2C} = \frac{x_g^*}{2}$ | $C = C_{\max} = 1.791$ $X^* = 0.1872$ |
| 3 CMCS | in No. 2 | in No. 2, Equations (16) and (19) | 0.9544 | in No. 2, Equations (18), (19) and (21) | in No. 2, Equations (20)–(22) | $C = 0.2$ $X^* = 0.2386$ |
| 4 CMC | $1 - \varepsilon_o = 0.5236$ | - | 1.00 | - | - | Equation (5), mono-fractions |

Slight differences in the values of the coefficients result from the fact that the line is determined from a different amount of data. For further considerations, we assume Equation (23).

4.3. Case 2—Increased Bulk Density of Fine Grains, Version A

In general, fine coal grains contain a higher mineral content than grains considered thicker. For a two-parameter line, Equation (15) is transformed into a form containing the constant term C_o

$$Y = CX + C_o \quad (25)$$

which has an analogous form as for Equation (13):

$$\rho = \frac{\pi}{6} \rho_o \frac{1 + C_o + Cx_g}{1 + Cx_g^2} \quad (26)$$

When $x_g = 1$, then

$$\rho_g = \frac{\pi}{6} \rho_o \left(1 + \frac{C_o}{1 + C} \right) \quad (27a)$$

and when $x_g = 0$, then:

$$\rho_d = \frac{\pi}{6} \rho_o (1 + C_o) \quad (27b)$$

which means the density of bulk densities of both fractions, still treated as coarse grains ($x_g = 1$) and fine ($x_g = 0$).

Analogously, formulas are obtained as before (for the constant term free (19) and (20), when $C_o = 0$):

$$\rho^* = \frac{\pi}{6} \rho_o \frac{C \sqrt{(1 + C_o)^2 + C}}{2 \left[C + \left((1 + C_o)^2 - (1 + C_o) \sqrt{(1 + C_o)^2 + C} \right) \right]} \quad (28)$$

for

$$x_g^* = \frac{\sqrt{(1 + C_o)^2 + C} - (1 + C_o)}{C} \quad (29)$$

In relation to forms (19) and (20), Equations (28) and (29) have a more complex form, but their use requires knowledge of the constant term C_o , which is determined experimentally.

4.4. Case 3—Increased Bulk Density of Fine Grains, Version B

Model (13) for suggestion (26) and previous considerations should be expressed as:

$$\rho = \rho_{\min} \frac{1 + Cx_g}{1 + Cx_g^2} \quad (30)$$

where

$$\rho_{\min} = \rho_d x_d + \rho_g x_g \quad (31)$$

which corresponds to linear additivity with respect to the proportion of coarse grains:

$$\rho_{\min} = (\rho_g - \rho_d) x_g + \rho_d, \quad \rho_d > \rho_g \quad (32)$$

For simplicity, the record (32) is presented in general numbers:

$$\rho_{\min} = -m x_g + n \quad (33)$$

The arrangement of function scales for the linear Equation (30) from (31) is analogous to Equation (14):

$$\frac{\rho_d}{\rho_{\min}} - 1 = Cx_g \left(1 - \frac{\rho_d}{\rho_{\min}} x_g \right) \quad (34)$$

and it is sensible to use only when we know the analytical form (32).

For further purposes, Equation (30) is combined with (33):

$$\rho = n \frac{1 + Cx_g}{1 + Cx_g^2} - mx_g \frac{1 + Cx_g}{1 + Cx_g^2} \quad (35)$$

Equation (35) will be used to determine if there is an upper limit to accepting values by the constant C , to determine the maximum function for the condition $d\rho/dx_g = 0$.

In case 1, the limit density was calculated according to the model (35) [19]:

$$z = \frac{\int_0^1 \rho dx_g}{\rho_0} \quad (36)$$

which after the performance of the actions leads to the equation (integral solutions are presented in Supplementary Materials):

$$z = \left[-m + (n + m) \frac{\arctg \sqrt{C}}{\sqrt{C}} + \frac{1}{2} \left(n - \frac{m}{C} \right) \ln(1 + C) \right] / \rho_0 \quad (37)$$

From the calculations, for example, for data from [10] for the planned experiment and air-dry ($W_t^r = 0\%$) dust fraction below 0.5 mm $\rho_d = 771 \text{ kg/m}^3$ and for the blend of 3 ÷ 5 mm and over 5 mm in the ratio 1:1 $\rho_g = 676 \text{ kg/m}^3$ we obtain $m = 95 \text{ kg/m}^3$ and $n = 771 \text{ kg/m}^3$.

For the maximum value of $C = 1.791$ acc. (37), $z = 0.673$ so a value greater than $z = 0.632$, which means that in dependence (30) the grain division constant will be smaller than that assumed by model (4) or (13).

However, for the condition $d\rho/dx_g = 0$, the model (30) in the order (35) has a maximum for the share of coarse grains:

$$x_g^* = \frac{\sqrt{C(1 + C)(Cn^2 + m^2)} - C(n + m)}{C(Cn - m)} \quad (38)$$

and for $m = 0$ we obtain Equation (20) again.

4.5. Analysis of the Literature Data

In-depth studies of bulk density determined in laboratory conditions by the Gekker-Mamuta method according to the planned experiment are presented in [10]. Rejecting boundary data for individual mono-fractions, for air-dry coals, and for grains with a moisture content of 8% (recalculated into air-dry state) is shown after transformation of data according to (14) by entering the locus (23)—Figure 4.

It should be noted that according to the plan of the experiment, we study grain systems composed of at least two grain fractions up to four fractions. They are, therefore, compositional systems and in the case of air-dry coals, it can be assumed that the results according to Figure 4a are in the majority of cases in the grains triangle, and for virtually all wet coals—Figure 4b. Going further from Figure 4, it follows that most of the measurement data lie on the locus (23) or focus on it, and thus the same experience indicates the maximum bulk density in some nodes.

On the other hand, the focusing of the measurement data along the straight line (25) is completely lost; it can even be assumed that there are very many lines with variable directional coefficients. Assuming the possibility of averaging, it can be assumed that for dry coals $C = 1.2$ and for wet carbon $W_{ex}^r = 8\%$, $C = 0.5$. The given values of the constant C have only an approximate meaning.

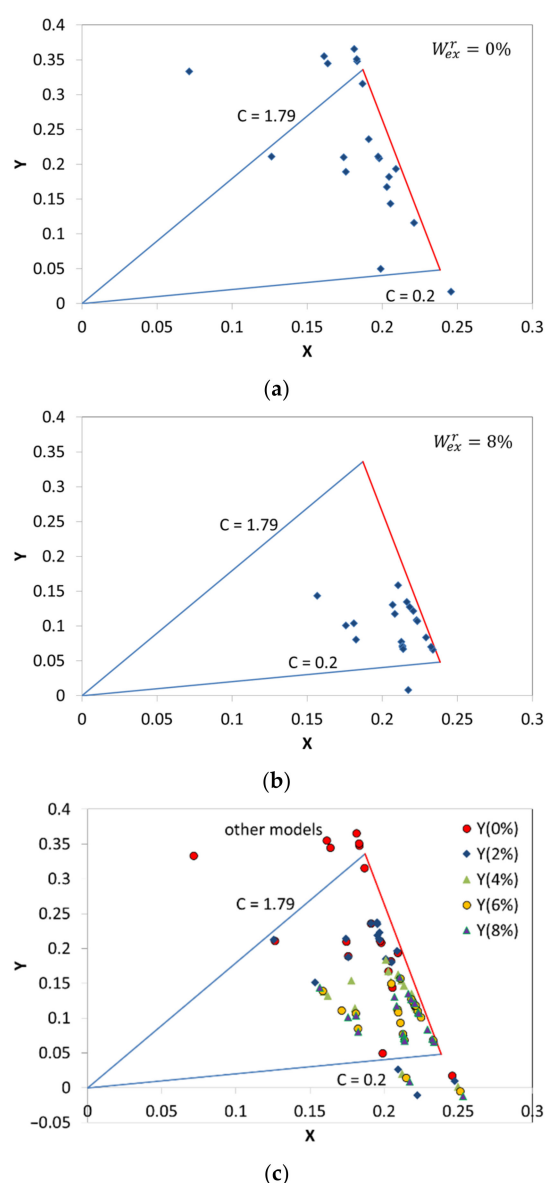


Figure 4. The arrangement of function scales for the triangle of grains of measurement data defining the bulk density obtained in the experiment planned according to [10] for: (a) $W_{ex}^r = 0\%$, (b) $W_{ex}^r = 8\%$, air-dry basis, (c) combined data for dla $W_{ex}^r = 0; 2; 4; 6; 8\%$ Source: authors own work.

The data presented in Figure 4 show that dry coals have a greater tendency to compact, but this is a more chaotic phenomenon than in the case of wet coals, which densify but at the level of much lower bulk densities.

Despite these constraints (which have been established for formula (24)), there is still the problem of how to interpret measurement data above $C > 1.791$, as is clearly shown in Figure 4a,c because the lower limit of $C = 0.2$ is a conventional issue and the fractions do not have to be compacted, when $C = 0$.

The conclusion is that if we use only one coordinate $[x_g; \rho]$ and formula (18) then high values $C = 2 \div 3$, or higher, probably suggest model (25) or (26) containing the constant term free $C_0 > 0$ (case 2, version A) or more complicated (30) from (27)—case 2, version B.

It cannot be ruled out that in the range of large shares of coarse grains ($0.8 < x_g < 1$), the grain sets are arranged in accordance with the approach in Equation (1a) (see Figure 5a).

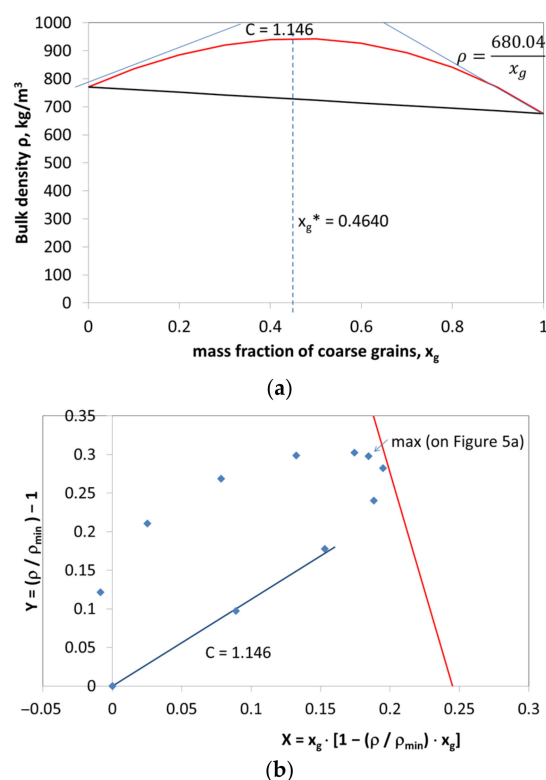


Figure 5. Data according to (39) in: (a) Cartesian coordinate system, (b) by model (34) taking into account linear additivity (32).

Another example can be generated from the same work [10] adopting a system of two fractions of coarse grains composed of grains 3 ÷ 5 mm and above 5 mm in a 1:1 ratio and fine grains below 0.5 mm ($W_{ex}^r = 0\%$) and given there the coefficients of polynomials.

For such a system of grains, the polynomial has the form:

$$\rho = -130.5x_g^3 - 679.5x_g^2 + 715x_g + 771, \text{ kg/m}^3 \quad (39)$$

with the condition $d\rho/dx_g = 0$, we obtain the maximum coordinates: $x_g^* = 0.4640$, $\rho^* = 943.43 \text{ kg/m}^3$.

Equation (39) describes changes in the bulk density of a system of two fractions: fine, below 0.5 mm and coarse, above 3 mm, using the 3rd degree polynomial. Under boundary conditions, it is the case when the bulk density of the fine fraction is higher ($\rho_d = 771 \text{ kg/m}^3$) than the coarse one ($\rho_g = 676 \text{ kg/m}^3$) and thus fits into case 3, version B.

Figure 5a shows the typical dependence of bulk density changes in (39), and Figure 5b transformation for the most complicated case in (34).

The results indicate that the curve is arranged according to several possibilities symbolically marked in Figure 5a. In the vicinity of fine grains, a constant $C = 1.15$ appears, and in the opposite environment, a large cluster of coarse grains has a maximum density in Equation (1a). The maximum is not described by the appropriate model, but works with a practical limitation—the locus (23).

It should be noted that in this case, the polynomial model (39) generated by the planned experiment (Figure 5a) was used, while the locus (23) was derived from the model (13). Thus, the polynomial Equation (39) implements several possibilities into one empirical approach.

5. Experimental

5.1. Own Research—Coarse Grains (Briquettes) Crushing Model for $D_g \gg D_d$

The simplest example of the formation of two grain sets with grain sizes clearly distant from each other may be the tests of crushing coal briquettes in the Shatter Test-type drop system. Crushing briquettes in drop cycle involves the formation of grain agglomerates that gradually disintegrate to the size of the grains from which they were formed. This causes free inter-grain spaces to be naturally filled.

Further research consists in determination of the bulk density of isomorphic briquettes of steam coal with the shape of a pillow with the dimensions $62.6 \times 66 \times 36$ mm ($W_t^r = 3.8\%$, $A^d = 15\%$, $NCV = 25.0$ MJ/kg, $\rho_o = 1380$ kg/m³—determined by the hydrostatic method).

Briquettes weighing approx. 92 kg were placed in a metal box with a volume of $V = 1.26$ m³ ($0.7 \times 0.4 \times 0.45$ m), and the crates were opened and briquettes dropped from a height of 1.5 m onto a steel plate. The bulk density of the briquette mixture was then determined. These activities were repeated 14 times, the whole crushed material was fed into the crate, and the entire cycle was repeated and the arithmetic means from two measurements were taken. Further discharges were interrupted when the proportion of briquettes (grains over 40 mm) was 70% ($x_g = 0.70$) and according to the limit given in Equation (1a) should be $x_g^* = (2 - \frac{\pi}{6})^{-1} = 0.677$.

5.2. Grinding of Coal Blends

Additional own research on the change in bulk density of the coal blend for the top charging system was carried out for the version of grinding its components and, in parallel, for the entire ternary coal blend. The coal blend was in an air-dry state, grain composition: >10 mm—5.3%, $5 \div 10$ mm—7.6%, $3 \div 5$ mm—10.3%, $1 \div 3$ mm—16.6%, $0.5 \div 1$ mm—18.3%, <0.5 —41.9% showed a bulk density of $\rho^d = 847.8$ kg/m³ (average of two measurements). Coal was ground in a laboratory device, the milling was carried out for 30 min, and every 5 min the bulk density was determined as the average of two measurements.

5.3. Moisture Content Impact

Coal samples from the Institute for Chemical Processing of Coal (IChPW) were sieved into the following grain classes: <0.5 mm, $0.5 \div 1$ mm, $1 \div 3$ mm, $3 \div 5$ mm, >5 mm, after drying to an air-dry state. Grain size of the blend is the effect of combining grain classes created approximately by the grain distribution function of the undersize, determined by the acronym GGS:

$$P = 100 \left(\frac{D}{D_{\max}} \right)^k, \% \quad 0.5 \leq D \leq 5 \text{ mm} \quad (40)$$

obtaining 21 samples, with the parameters: exponent $k = 0.30 \div 0.73$ and $D_{\max} = 4.5 \div 26.0$ mm.

It was assumed that for some parameters, the GGS functions of the undersize show maximum density, as exemplified by the Fuller curve, giving up the creation of coal blend using shares resulting from the RRSB function. The control tests of grain distributions in many cases proved different than expected: the coefficient of determination turned out to be low in the range of $r^2 = 0.93 - 0.97$ (13 grains per 21).

For all samples, bulk density measurements were made at the total moisture content $W_{ex}^r = 4\%$ and 10% .

5.4. Influence of the Coal Blend Density with Similar Qualitative Composition on the Coke Quality Indexes

The coal blend used in the top charging system was selected for the tests, with a composition according to PN-G-97002: 1982P as presented in Table 4.

Hard coking coals were a blend from three mines, similar to semi-soft coking coals. Samples weighing 4 kg for tests in the Karbotest installation [20] were prepared as follows.

Air-dried coals were divided into the following grain classes: <0.5 mm, 0.5 ÷ 1 mm, 1 ÷ 3 mm, 3 ÷ 5 mm, >5 mm. Individual grain classes of the coal blend were composed from the scattered fractions by combining them, maintaining a constant quantitative ratio in the given types of coal. Thus, five new coal mixtures were obtained with very similar coking properties to the initial blend, Table 5.

Table 4. Coal blend composition.

| | |
|--|------|
| Hard coking coals (Polish coal classification 35.1) | 63% |
| Hard coking coals (Polish coal classification 35.2B) | 16% |
| Semi-soft coking coals (Polish coal classification 34) | 21% |
| | 100% |

Table 5. Coking properties of coal blend with a constant qualitative composition with moisture content $W_t^r = 10\%$.

| Parameter | Unit | Value |
|-----------|------|-------|
| W_t^r | % | 1.3 |
| A^d | % | 7.4 |
| V^{daf} | % | 28.12 |
| RI | % | 75 |
| SI | - | 8 |
| t_I | °C | 393 |
| t_{II} | °C | 440 |
| t_{III} | °C | 490 |
| A | % | 28 |
| B | % | +59 |
| t_1 | °C | 394 |
| t_{max} | °C | 447 |
| t_3 | °C | 487 |
| F_{max} | ddpm | 515 |

The coking process was performed in the Karbotest installation described in previous works [20,23,24]. Obtained coke samples were analysed to obtain CRI and CSR results acc. ISO 18894:2006(E).

6. Results

6.1. Coarse Grain Crushing, $D_g \gg D_d$

The results of the tests described in Section 5.1. are presented as follows. The bulk density increase amounted to 48.2% from the level of 730.1 kg/m³ to 1081.7 kg/m³. Obtained results are practically in line with formula (3) in the final phase of the experiment where the maximum density was obtained.

This example illustrates the real practical possibilities; densification by crushing ends with compliance with the record (3) or (7); further saturation of free spaces according to Equations (8)–(10) does not take place.

From the technological point of view, in the coking industry with the top charging system, it is sensible to crush whole briquettes, but not in the 100% crushing version to approx. 70%, because this variant is biased with too high saturation of costly mechanical activities, as well as increased coking time.

Tests results are illustrated in Figure 6, where the determined correlation line satisfies the left branch CMC Equation (1a) with a sufficiently consistent true density (1380 kg/m³ determined, 1415.3 kg/m³, relative error 2.6%).

6.2. Grinding of Coal Blends, $D_g \rightarrow D_d$

Referring to Section 5.2, the graphical representation of the obtained results in the function scale system (14) is illustrated in Figure 7.

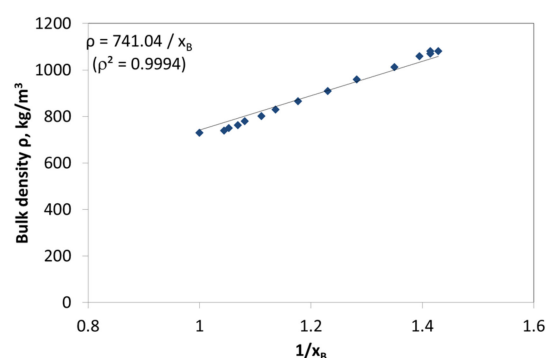


Figure 6. Bulk density of crushed briquettes after Shatter Test drop tests against the inverse yield of briquettes above 40 mm.

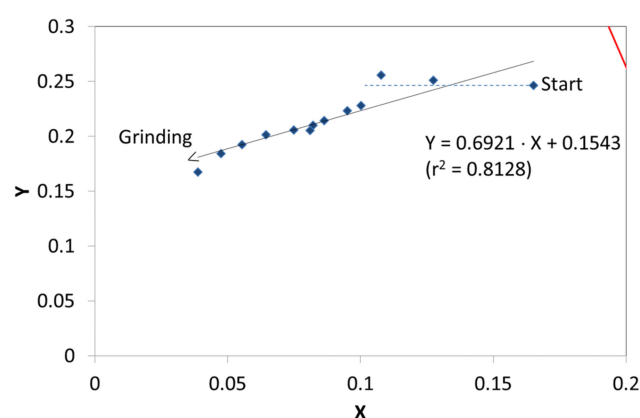


Figure 7. Triangle grain size for crushed coal blend—converted to air-dried state from wet base $W_{ex}^T = 8\%$.

With the milling time, the bulk density decreases. However, the bulk density does not change initially. The adopted milling method does not affect the formation of bulk density changes. While the initial coal blend has a high bulk density ($\rho^d = 847.8 \text{ kg/m}^3$) and with $C = 1.49$, the bulk density decreases with the milling time and this is accompanied by a reduction to $C = 0.69$ and at the same time constant term free appears.

The example at least partially indicates the importance of the model (13) assuming that the whole time, the coarse and fine grains system is the same grain class.

In some approximation, coarse grains crumble into identical fine grains, whereby the constant C changes only slightly.

It can be shown that the appearance of the C_0 has no effect on the locus (23), which symbolically is shown in Figure 8. Comparing the model for $C = 0.69$ acc. Equation (13) and for the constant term free $C_0 = 0.15$ in Equation (26) and making the transformation acc. (14), we obtain two straight lines whose maximum values are close to the locus (23) on which the maximum values are located.

Any coordinate $[x_g; \rho^d]$ after transformation according to Equation (17) to the position $[X; Y]$ and located in the area of the grain size triangle (Figure 3b) indicates two possibilities, either Equation (13) or Equation (26) is fulfilled. The most important, however, is the visual assessment of the distance from the locus (23) to this coordinate.

Model (26) is especially useful when we analyse grain size distributions below the maximum value.

The presented considerations are a suggestion for the real conditions to accept the model (13) in a form without a constant term free, implementing variable values in edge nodes in it.

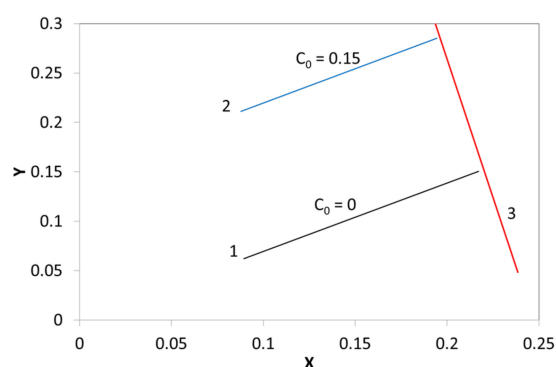


Figure 8. Data for model (13) and constants $C = 0.69$ and $C_0 = 0$ and 0.15 after transformation acc. (14) from locus (23) for $0.1 \leq x_g \leq 0.5$, $\rho_o = 1300 \text{ kg/m}^3$. 1—acc. (13), $\rho = \frac{\pi}{6} \rho_o \frac{1+0.69x_g}{1+0.69x_g^2}$, $x_g^* = 0.4348$, $\rho^* = 784.02 \text{ kg/m}^3$. 2—acc. (26), $\rho = \frac{\pi}{6} \rho_o \frac{1.15+0.69x_g}{1+0.69x_g^2}$, $x_g^* = 0.3893$, $\rho^* = 874.20 \text{ kg/m}^3$. 3—locus Equation (23).

6.3. Moisture Content Impact

The relationship between the bulk density and the moisture content is generally known, and it is a curve of at least 2 degrees showing a minimum (e.g., [19]). In relation to the tests indicated in Section 5.3, a different approach is presented, including the dispersion of the constant C in the field of the triangle of grains. The grain size triangle is shown in Figure 9.

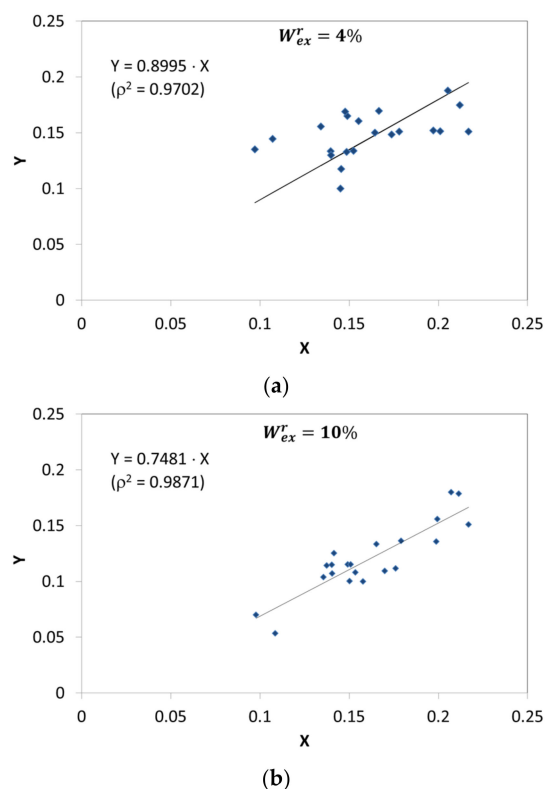


Figure 9. Triangle grains for grain distributions close to the maximum density and for two levels of moisture content recalculated into air-drying basis: (a) 4%, (b) 10%.

Coal containing 4% and 10% moisture meets model (13). However, for 4% moisture, the fluctuation of the $C = 0.90 \pm 0.035$ constant is too high ($C = 0.7 \div 1.45$) to consider this case satisfactory. A much more sensible case is the case of wet coals (10%), where the

compaction susceptibility is $C = 0.75 \pm 0.019$ but still does not reach the maximum values consistent with the locus (23).

6.4. Influence of the Coal Blend Density with Similar Qualitative Composition on the Coke Quality Indexes

The coking process results described in Section 5.4 graphically are presented in Figure 10. Figure 10a shows the grain size triangle according to the functional scales of Equation (14) together with the locus (23). The constant C was determined individually according to Equation (14). From a statistical point of view, according to the t -test, the equations given in Figure 10a are significant at the level of $sl = 0.012$ ($Y = 1.59X - 0.17$) and $sl = 0.0$ ($Y = 0.75X$), which authorizes the adoption of the model (14) as more justified. This fact makes it possible to adopt in this range the mean grain distribution constant equal to $C = 0.75$ (arithmetic mean $C = 0.726$).

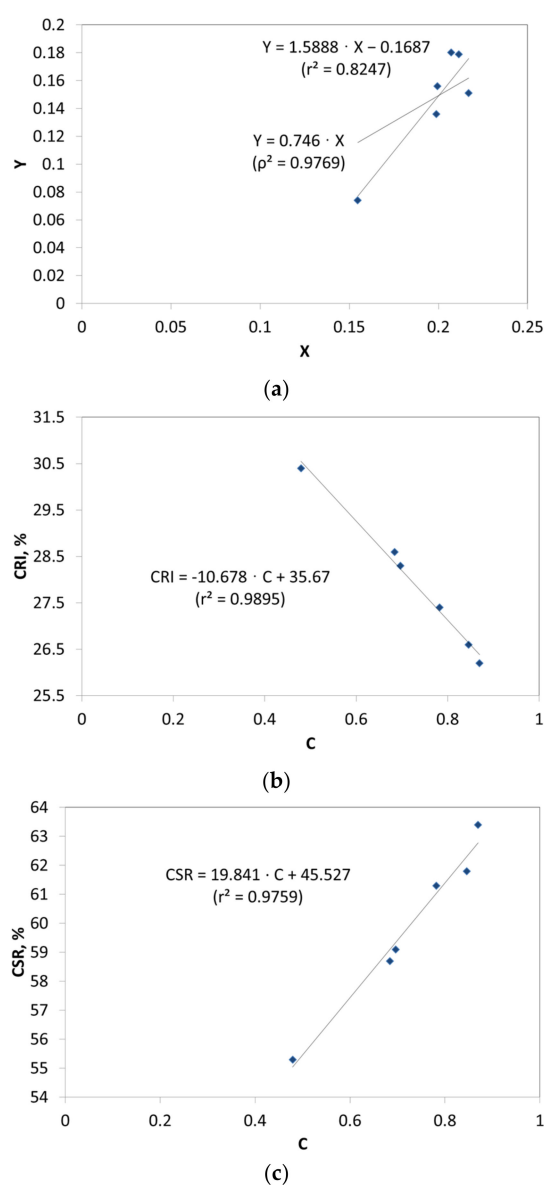


Figure 10. Coke quality parameters dependent on grain distribution constant: (a) C for $D_g = 3$ mm grain triangle acc. (14), (b) CRI vs C , and (c) CSR vs C .

The constant C determined at each coordinate shows an effect on the quality of coke, i.e., on CRI (Figure 10b) and CSR (Figure 10c).

The point marked in Figure 10a with the coordinates $X = 0.155$, $Y = 0.074$ ($C = 0.48$) corresponds to the lowest coke quality (CRI = 30.4% (Figure 10b) and CSR = 55.3% (Figure 10c)).

The obtained grain compositions with a constant quality of the coal blend clearly indicate a linear relationship between the CRI/CSR indexes and the calculated grain constant C . As also results from Figure 10a, the next two or even three carbon mixes, due to the grain composition, already reach the locus (23).

The grain size triangle used in designing a composition of coal blends was still used. An example for initiating comprehensive research is related to the practical use of this method for industrial purposes.

The issues of making a composition of coal blends for a top charged system should take into account the optimal selection of the grain composition [1,2,7–9,17–19]. In the case of a fixed composition, an extremely important element is to control the consistency of the degree of moisture and grain composition, at least in terms of analysing the proportion of fine grains, which usually means monitoring the proportion of grains below 0.5 mm.

In a specific case, a coal blend with a maximum moisture content of $W_t^T = 8\%$ is used, with the following composition:

Hard coking coal (type 35.1)—74%, semi-soft coking coal (type 34)—26%.

The problem to be solved is the introduction of more semi-soft coking coals without significantly deteriorating the quality of the coke.

Figure 11 shows the results of research on the properties of coals supplied from various mines. In this case, there are 19 samples, and against this background the properties of the starting blend and three proposals for changed qualitative compositions were entered. Table 5 presents the basic data for these four blends.

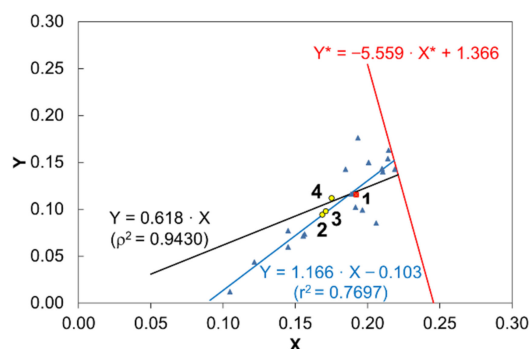


Figure 11. Deliveries of hard and semi-soft coking coals in the system of scales of the grain size triangle, number of samples 19, with the properties of the starting blend and changed qualitative compositions marked.

As in the previous example, coke from coal blends was obtained from the Karbotest installation, and the CRI/CSR indices were determined for the obtained coke.

It should be noted that the Y component is a relative increase in the bulk density in relation to the hypothetical level of $\rho = \frac{\pi}{6}\rho_o = 680.7 \text{ kg/m}^3$. Basic data for 19 coal deliveries in the triangle grain size layout indicate a very unfavourable system for changes in the rational grain size distribution. The most abundant hard coking coal (74%) is on the locus line (23). In light of the considerations presented also in this work, it is logical to confirm that their fragmentation and the introduction of new components to the optimal grain composition of hard coking coals lowers the bulk density, and this effect will be increased when the introduced coals are more finely ground.

Thus, each added grain composition of the lower rank coal will move away from this line constituting Equation (23), and at the same time the coking properties will decrease. Indeed, coal blend, considered to be the starting one, changes its position when changing the qualitative composition, and these changes are better described by the line with the equation $Y = 0.618X$ than by $Y = 1.166X - 0.103$. In both cases, both lines can be considered adequate at the statistical level of the t -test, 0.0 (4) and 0.0 (5), respectively.

The 6% reduction in the share of hard coking coals (Table 6) solves this problem at the level of the reduced coke quality, which is acceptable in this case.

Table 6. Coordinates of coal blends and coke quality.

| No | Coals, Type 35.1/34 | X | Y | C acc. (14) | CRI, % | CSR, % | Remarks |
|----|------------------------|-------|-------|-------------|--------|--------|-----------------------|
| 1 | 74% 26% | 0.192 | 0.115 | 0.599 | 29.1 | 57.8 | standard coking blend |
| 2 | 74% 26% | 0.169 | 0.095 | 0.562 | 32.0 | 53.0 | type 34 shredded |
| 3 | 68% 32% | 0.171 | 0.098 | 0.573 | 32.2 | 52.0 | - |
| 4 | 62% 38% | 0.175 | 0.112 | 0.64 | 33.3 | 50.2 | - |

Figure 10b,c suggests very strong relationships between the coke quality and the constant C. The higher its value (here at $C = 0.9$), the higher the quality of CRI/CSR values provided. In order to ensure greater credibility of the obtained results, 5 mm split grain size was adopted for consideration. A graphical illustration is given in Figure 12.

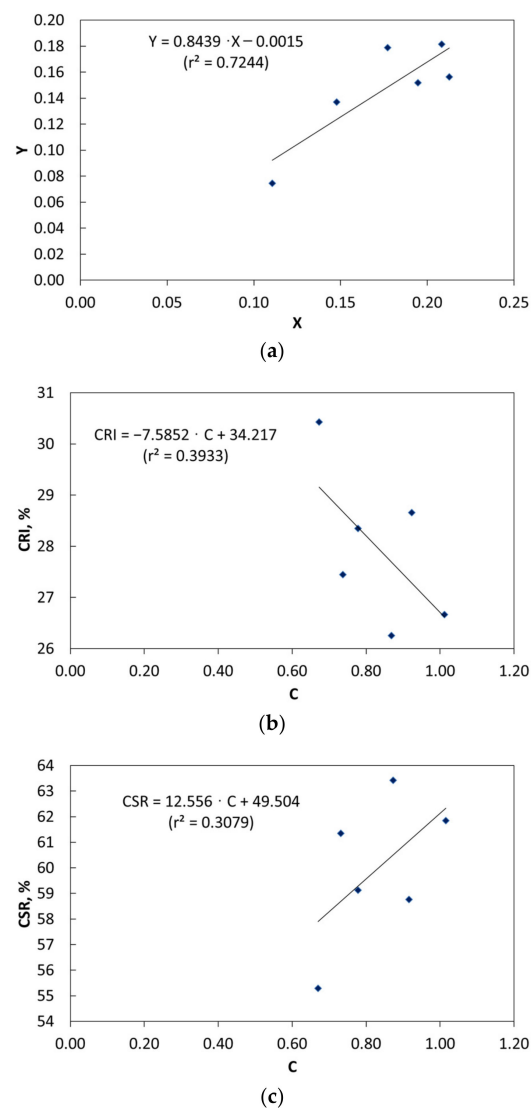


Figure 12. Coke quality dependence of grain distribution constant, C for $D_g = 5$ mm: (a) grain triangle acc (14), sl = 0.0316, (b) CRI vs C, and (c) CSR vs C.

The correlations are much weaker than in the case of the commonly used technological guideline, taken as the number of grains larger/smaller than 3 mm. On Figure 12c by conventional criteria, these correlations are considered to be not statistically significant, although the trend of change was followed as in Figure 10c. In the case of 5–10 mm coarse grains, it seems that their number is too small, as it amounts to 12.8–37.7%.

7. Summary

Expanding the possibilities of using grain distributions for coking purposes in accordance with the proposal Equations (1) and (4), it was found that CMC and CMCS models are the starting point for solving practical problems. The arrangement of two sets of grains, defined without validation as fine and coarse grains, CMC is represented by the model (1a) from (1b) while the distribution constant of grains C is characteristic of the CMCS model (13).

In the latter, three cases for CMCS were distinguished:

Case 1—triangle of grains limited by the locus (23), bulk densities of both fine and coarse fractions are identical and equal to $\rho = \frac{\pi}{6} \rho_0$;

Case 2—version A, Equations (25) and (26), bulk densities of these fractions are equal acc. Equation (27a,b);

Case 3—version B, Equations (30) and (31), the bulk densities of these fractions form the law of linear additivity (31), defined here as the minimum bulk density.

The presented material shows that grain systems can be described by several models in the full range of grain shares. Often, in the range of coarse grains, model systems described by Equation (1a) may form, as well as in the range of fine grains with a defined value of the constant C, which should not exceed the value of $C = 2$.

The basic message of this work is the proposal of the grains triangle, illustrated in Figure 3b, which limits the values assumed by the relations: bulk density—share of coarse grains/fine grains, for different levels of moisture content.

Each system of changing shares of coarse and fine grains is characterised by a constant C, but there is no need to determine it, especially from one coordinate $[x_g; \rho]$ according to formulas (14) or (34): it is sufficient to analyse whether the condition (24) is fulfilled. The compliance of the calculated value ρ with ρ^* means that the given grain set has reached its maximum density. The example shown in Figure 4, according to Equation (39), assumes there are three mechanisms: the grains triangle (Figure 5b) indicates a high probability of reaching the maximum density. It should be noted, however, that the locus (23) is derived from (13) and therefore from the theoretical model and for $\rho_0 = 1300 \text{ kg/m}^3$.

From these considerations, it follows that C should be more appropriately named susceptibility to model compaction. It does not have to be determined, because the locus (23) is a limitation.

The derived models or the grain size triangle enable the study of processes used in industry, mainly in coking and mining, for mechanical grain grinding. In the case of crushing coal briquettes for top charged systems, it is described by Equation (1a), while the grinding of coal blend is useful by Equation (25) or directly by Equation (13), or for more data—the grain size triangle.

Continuing the technological research, it was found that there is a very favourable linear correlation between the coke quality (CRI/CSR indexes) and the grain division constant C, when we accept 3 mm as a split grain size, compared with other possibilities in this regard.

Although for high-quality cokes there is a very reliable linear correlation between the CRI/CSR indices (Figure 1 in [25]), according to the presented study, the number of factors determines the CSR index, and its value is compensated by the reactivity of the CRI coke (Figure 3 in [25]). This is the reverse sequence to the assay procedure in the order where the CSR parameter is obtained after CRI is determined. Results of this work as well as [7] for the same coal blend show that changes only in grain size distribution influence the reactivity index (CRI) more than the strength after reaction index (CSR).

The homogeneity of the coking properties depends not only on the degree of compaction of the coal charge containing semi-soft coals with specific grain sizes, but above all on the hard coal coking ability. The maximum compaction may occur for too high a share of coarse grains with poor coking ability.

The relations resulting from the achievement of the maximum compaction (Equation (23)) suggest that coal deliveries to coking plants force them to crush and thus lower the bulk density of charge (e.g., Figure 11). On the other hand, there is still a need to use hard coking coals with very good coking properties in order to increase the share of semi-softs coal in the blend so as not to increase the reactivity of the coke.

8. Conclusions

- A coordinate system was proposed to analyse the relationship between bulk density and the share of grains considered coarse. Such a diagram was named the triangle of grains, and the most important element is the locus (23). Any coordinate $[x_g; \rho_d]$ after transformation according to Equation (17) to position $[X; Y]$ and located in the area of the graining triangle (Figure 3b) is the simplest visualisation of the distance from the maximum density determined by the locus (23). It is a new element in the analysis of the grain composition properties for the coke industry, especially for the top charging system or mining.
- The C constant present in the CMCS model should be in the $C < 2$ range; the higher the moisture, the lower its value. However, in the case of dry grains, there may be several densification models, so there is no reason to attribute this constant of universality.
- In practice, the CMC model meets the description of compacting coarse grains with fine grains acc. Equation (1a), in the range from 0.8 to approx. 1.0 shares of coarse grains. In the case of the CMCS model, three cases were identified that are dependent on the bulk density of coarse and fine grains in relation to the expression $(\pi\rho_o/6)$. It was found that they may be equal: fine grains have a higher bulk density than coarse grains, and both grain sets meet the law of linear additivity in the absence of compaction.
- From the presented considerations and examples, it follows that C should have a more appropriate name: the coefficient of susceptibility to model compaction. It does not have to be determined, because the locus (23) is a limitation.
- There is a linear relationship between the coke quality parameters and the grain separation constant C, calculated from formula (14) assuming the separation grain size of 3 mm for coarse grains.

Supplementary Materials: The following are available online at <https://www.mdpi.com/article/10.3390/en14133911/s1>, Equations (S1)–(S5).

Author Contributions: Conceptualization, A.M.; Methodology, A.M., B.M. and M.Ś.; Software, B.M.; Validation, A.M. and M.Ś.; Formal Analysis, A.M.; Investigation, B.M.; Resources, A.M. and B.M.; Data Curation, A.M.; Writing—Original Draft Preparation, A.M.; Writing—Review & Editing, A.M. and B.M.; Visualization, A.M. and B.M.; Supervision, M.Ś.; Project Administration, B.M.; Funding Acquisition, B.M. All authors have read and agreed to the published version of the manuscript.

Funding: This research was co-financed by the European Union from funds under the Program Intelligent Development. Project implemented as part of the National Centre for Research and Development competition POIR.01.02.00-00-0209/17-00.

Data Availability Statement: Data available on request due to restrictions eg privacy or ethical.

Conflicts of Interest: The authors declare no conflict of interest.

Nomenclature

| | |
|----------------------|--|
| $a = 6/\pi\rho_o$ | Equation (18) |
| A^d | ash content, dry state (%m/m) |
| C | grain distribution constant, and in this paper also: coefficient of susceptibility to compaction |
| C_o | intercept in Equation (25) |
| D | grain diameter (mm) |
| f | shape coefficient, $f \geq 1$, for a sphere $f \equiv 1$ |
| k | exponent in Equation (40) |
| n, m | parameters of straight equation in Equation (33) |
| p | exponent in Equation (10) |
| P | part by weight of grains smaller than size D (%) |
| r^2, ρ^2 | determination coefficients for the double and single parameters of the straight equation |
| sl | significance level |
| x | mass fraction |
| X | new independent reversible variable |
| Y | new dependent variable, also $Y = \frac{\Delta\rho}{\rho}$ |
| W_{tr}^r, W_{ex}^r | content of total and transitory moisture (%) |
| z | boundary compression Equation (36) |
| ρ | bulk density (kg/m^3) |
| ρ_o | true density (kg/m^3) |
| $\Delta\rho/\rho$ | relative bulk density increase |
| ε | porosity |
| ε_o | porosity of isomorphous spheres, $\varepsilon_o = 1 - \frac{\pi}{6} = 0.4765$ |
| <i>Subscripts</i> | |
| B | briquettes |
| d | fine size grains |
| g | coarse size grains |
| \max | maximum |
| \min | minimum |
| <i>Superscripts</i> | |
| d | dry |
| $*$ | maximum of function |
| <i>Abbreviations</i> | |
| CMC | Curve of Maximum Compression |
| CMCS | Curve of Maximum Compression with regard to Separation effects |
| CRI, CSR | Coke Reactivity Index, Coke Strength after Reaction |
| GGG | Gates–Gaudin–Schuhmann function |
| NCV | net calorific value |
| RRSB | Rosin–Rammner–Sperling–Bennett function |

References

1. Rejdak, M.; Strugała, A.; Sobolewski, A. Stamp-Charged Coke-Making Technology—The Effect of Charge Density and the Addition of Semi-Soft Coals on the Structural, Textural and Quality Parameters of Coke. *Energies* **2021**, *14*, 3401. [\[CrossRef\]](#)
2. Żarczyński, P.; Strugała, A. Studies on the Possibility of Extending Coal Resources for Coke Production through the Application of Coal Predrying. *Energy Fuels* **2018**, *32*, 5666–5676. [\[CrossRef\]](#)
3. Díez, M.A.; Alvarez, R.; Cimadevilla, J.L.G. Briquetting of carbon-containing wastes from steelmaking for metallurgical coke production. *Fuel* **2013**, *114*, 216–223. [\[CrossRef\]](#)
4. Fernández, A.M.; Barriocanal, C.; Díez, M.A.; Alvarez, R. Influence of additives of various origins on thermoplastic properties of coal. *Fuel* **2009**, *88*, 2365–2372. [\[CrossRef\]](#)
5. Sharma, M.K.; Chaudhuri, A.J.; Prasad, S.; Prasad, B.N.; Das, A.K.; Parthasarthy, L. Development of New Coal Blend Preparation Methodologies for Improvement in Coke Quality. *Coal Prep.* **2007**, *27*, 57–77. [\[CrossRef\]](#)
6. Mianowski, A.; Sobolewski, A.; Janusz, M. *Partial Briquetting from the Perspective of “Smart Soko Plant” Project (Częściowe Brykietowanie Wsadu z Perspektywy “Inteligentnej Koksowni”)*; Institute for Chemical Processing of Coal: Zabrze, Poland, 2014.
7. Sobolewski, A.; Rejdak, M.; Czaplicki, A.; Janusz, M.; Mianowski, A. The effect of coal charge preparation on coke quality. *Chem. Ind.* **2014**, *93*, 2103–2110. (In Polish) [\[CrossRef\]](#)
8. Lyalyuk, V.P.; Sheremet, V.A.; Kekukh, A.V.; Otorvin, P.I.; Pizar, S.A.; Uchitel, A.D.; Lyahova, I.A.; Kassim, D.A. Rational Crushing of Coal Charge for Improvement of Coke Quality for Blast-Furnace Smelting. *Metall. Min. Ind.* **2010**, *2*, 81–86.

9. Sobolewski, A.; Klejnowski, K.; Łusiak, T.; Morel, J.; Olczak, C.; Ściażko, M.; Tatara, A.; Fitko, H.; Sobala, Z.; Korczak, J.; et al. *Smart Coke Plant Fulfilling Requirements of Best Available Techniques (Inteligentna Koksownia Spełniająca Wymagania Najlepszej Dostępnej Techniki)*; Project Report; IChPW: Zabrze, Poland, 2010. (In Polish)
10. Strugała, A. Badania modelowe gęstości nasypowej wsadu węglowego w aspekcie doboru optymalnego uziarnienia. *Koks Smoła Gaz* **1981**, *26*, 199–203. (In Polish)
11. Simonis, W. Mathematische Beschreibung der Hochtemperatur Verkokung von Kokskohle im Horizontalkammerofen bei Schüttbetriebs. *Glückauf Forsch.* **1968**, *29*, 103–119.
12. Simonis, W.; Rubrecht, E. Optimaler Körnungsaufbau von Kokskohle. *Glückauf Forsch.* **1965**, *26*, 301–308.
13. Klešnin, A.A.; Kuprin, A.I.; Klešnina, G.V. Vlijanie granulometričeskovo sostava i vlažnosti na poroznost' zernistych smesej. *Koks Chim.* **1967**, *3*, 1–8. (In Russian)
14. Kuprin, A.I.; Klešnin, A.A.; Klešnina, G.V. Zakonomernosti izmenenija poroznosti zernistych materialov i jeje opredelenije. *Stroit. Archit.* **1967**, *6*, 78–82. (In Russian)
15. Kuprin, A.I.; Klešnin, A.A. Izmenenije poroznosti' zernistych sred. *Koks Chim.* **1980**, *10*, 10–11. (In Russian)
16. Strugała, A. Matematyczny opis zageszczenia mieszanek węglowych, Part I. *Karbo Energochemia Ekol.* **1994**, *39*, 239–246. (In Polish)
17. Strugała, A. Matematyczny opis zageszczenia mieszanek węglowych, Part II Modele empiryczne. *Karbo Energochemia Ekol.* **1995**, *40*, 11–19. (In Polish)
18. Strugała, A. Packing density of non-randomly mixed solid particles. *Acta Mont. IRSM AS CR Ser. B* **2001**, *11*, 105–115.
19. Mianowski, A. Einfluß von Mahlgrad und Feuchtigkeitsgehalt der Kohlenmischung auf deren Schüttdichte. *Aufbereit. Tech.* **1989**, *7*, 434–442, (In German and English).
20. Mertas, B. Mass and Elements Balance of Polish and Czech Hard Coal Pyrolysis Process. *Solid Fuel Chem.* **2019**, *53*, 418–425. [[CrossRef](#)]
21. Feng, Y.T.; Han, K.; Owen, D.R.J. Filling domains with disks: An advancing front approach. *Int. J. Numer. Methods Eng.* **2003**, *56*, 699–713. [[CrossRef](#)]
22. Bryczkowski, A. *Testing of Grain Size Distribution Influence on Coke Quality (Badanie Wpływu Uziarnienia Mieszanek Węglowych na Jakość Koks)*; Czaplicki, A., Bigda, R., Bryczkowski, A., Stelmach, S., Lajnert, R., Figa, J., Eds.; IChPW: Zabrze, Poland, 2005. non-published work. (In Polish)
23. Piechaczek, M.; Mianowski, A. Coke optical texture as the fractal object. *Fuel* **2017**, *196*, 59–68. [[CrossRef](#)]
24. Rejdak, M.; Bigda, R.; Wojtaszek, M. Use of Alternative Raw Materials in Coke-Making: New Insights in the Use of Lignites for Blast Furnace Coke Production. *Energies* **2020**, *13*, 2832. [[CrossRef](#)]
25. Díez, M.A.; Alvarez, R.; Barriocanal, C. Coal for metallurgical coke production: Predictions of coke quality and future requirements for cokemaking. *Int. J. Coal Geol.* **2002**, *50*, 389–412. [[CrossRef](#)]